Multiple layer local oxidation
for fabricating semiconductor nanostructures

M. Sigrist[1], A. Fuhrer[1], T. Ihn[1], K. Ensslin[1], D. C. Driscoll,[2] and A. C. Gossard[2]

[1]*Solid State Physics, ETH Zürich, 8093 Zürich, Switzerland*
[2] *Materials Department, University of California,*
Santa Barbara, CA 93106, USA

(Dated: September 6, 2018)

Coupled semiconductor nanostructures with a high degree of tunability are fabricated using local oxidation with a scanning force microscope. Direct oxidation of the GaAs surface of a Ga[Al]As heterostructure containing a shallow two-dimensional electron gas is combined with the local oxidation of a thin titanium film evaporated on top. A four-terminal quantum dot and a double quantum dot system with integrated charge readout are realized. The structures are tunable via in-plane gates formed by isolated regions in the electron gas and by mutually isolated regions of the Ti film acting as top gates. Coulomb blockade experiments demonstrate the high quality of this fabrication process.

Optical lithography and electron beam lithography are the standard techniques to pattern tunable semiconductor nanostructures. A number of patterning techniques based on scanning force microscopes (SFMs) have been developed [1, 2, 3, 4, 5, 6, 7, 8, 9, 10, 11, 12, 13, 14, 15, 16, 17, 18, 19]. An especially useful technique is to oxidize substrates locally by applying a negative voltage between the SFM tip and the substrate. Sophisticated nanostructures can be fabricated, for example, on shallow Ga[Al]As heterostructures [8, 9, 10, 11, 12, 13]. The two-dimensional electron gas is depleted below oxide lines leading to mutually isolated regions of electron gas. The main experimental parameters influencing the oxidation process are the relative humidity of the environment, leading to a thin water film on the substrate surface, and the magnitude of voltage applied to the tip.

A similar oxidation technique has been used to divide thin Titanium films into areas mutually isolated by oxide lines [14, 15, 16]. Metallic single-electron transistors fabricated with this technique have been reported to show the Coulomb-blockade effect [17]. Local titanium oxidation has also been used on Ga[Al]As heterostructures with a thin Ti top gate film for defining self-aligned split-gates. On the application of appropriate gate voltages, a quantum point contact (QPC) was formed showing clear conductance quantization [9, 18].

As the size of nanostructures to be defined with these techniques becomes comparable with the full width of the oxide lines of typically 150 nm and the desired degree of control of individual parts of the structure requires more and more gate electrodes, neither local oxidation of the GaAs surface nor that of a titanium top gate alone meets the needs. The limits are of geometrical nature and imposed by the restriction of patterning only within the two-dimensional plane of the Ti or GaAs surface. Therefore, a patterning technique is desirable that makes the third spatial dimension accessible. One option is the use of local oxidation on the surface of the semiconductor, fol-
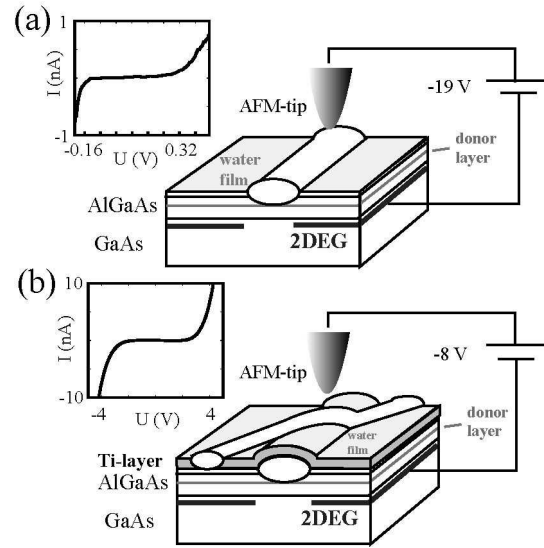
FIG. 1: (a) Schematic of the GaAs-oxidation step. Local oxidation of the GaAs surface depletes the electron gas locally below the line. The inset shows the current between separated regions of the 2DEG measured at 4.2 K. (b) A thin Ti film is evaporated and oxidized using a voltage biased SFM-tip. The inset shows the current between separated regions of the film measured at a temperature of 4.2 K.

lowed by the deposition of top gates defined with electron beam lithography techniques [19]. In this approach the alignment of the top gates with SFM-defined structures has to be achieved using another electron beam lithography step prior to the local oxidation for the definition of markers on the surface.

In this letter, we demonstrate an approach where the alignment of the top gate structures with the previous oxide structure in GaAs is achieved using a SFM. Our method combines the direct oxidation of a Ga[Al]As heterostructure (first step) with the subsequent evaporation of a thin titanium gate (second step) which is then pat-

terned using the local oxidation technique with the SFM (third step). We demonstrate the fabrication technique with the realization of a four-terminal quantum dot (sample A) and a double-quantum dot with integrated charge read-out (sample B). The occurrence of Coulomb blockade demonstrates the high quality and stability of the structures. The tuning possibilities of the nanostructures are significantly increased by the metallic Ti gates on top and their alignment with the nanostructure is straightforward.

The fabrication process is based on high-quality Ga[Al]As heterostructures containing a two-dimensional electron gas (2DEG) 34 nm and a back gate 1.4 μm below the surface. A 22×22 μm^2 mesa with Ohmic contacts and metallic top gate fingers for contacting the Ti film are defined by photolithography.

In the first step the nanostructure is defined by direct oxidation of the GaAs surface using the voltage-biased tip of a SFM in a humidity-controlled environment. The resulting oxide lines deplete the electron gas below [Fig. 1 (a)]. Typical break down voltages across an oxide line in the 2DEG are a few hundred mV at liquid He temperatures [an example is shown in the inset of Fig. 1 (a)]. Details of this fabrication step are described in Refs. 12 and 16. In the second step (using electron beam lithography), we define a 22×22 μm^2 mask overlapping all the top gate fingers and evaporate a 6-7 nm thick titanium film. The metal layer on the resist is stripped with a lift-off process. The resistivity of the remaining Ti film is of the order of 10 kΩ and the surface roughness is 1-2 nm peak-to-peak which is important for further structuring. A Schottky barrier forms between the heterostructure and the Ti film allowing its use as a top gate.

In the third step, the top gate is split into regions of dedicated functionality by oxidizing the Ti film locally, again with the voltage-biased tip of the SFM as shown in Fig. 1 (b). Since we have not found a clear selectivity between the oxidation process of GaAs and that of Ti for any humidity or tip bias parameters, the writing parameters are chosen carefully, such that the 2DEG density is not measurably reduced by the Ti lithography on top of the GaAs-structure. For the Ti oxidation process, the SFM is operating in tapping mode controlled by a standard feedback loop. The relative humidity at room temperature is kept constant at (43 ± 0.5) percent. A voltage of -7 to -9 V between SFM tip and Ti film oxidizes the Ti film locally without affecting the GaAs surface significantly. A control parameter for this process is the (averaged) height of the Ti oxide lines which further increases when the GaAs below the Ti film starts to be oxidized for voltages below -10 V. We found that lines of 2-3 nm height and 100 nm width isolate regions in the Ti film at low temperatures with typical break down voltages of a few Volts [inset of Fig. 1 (b)]. More details about the local Ti oxidation technique are found in Refs. 9, 15.
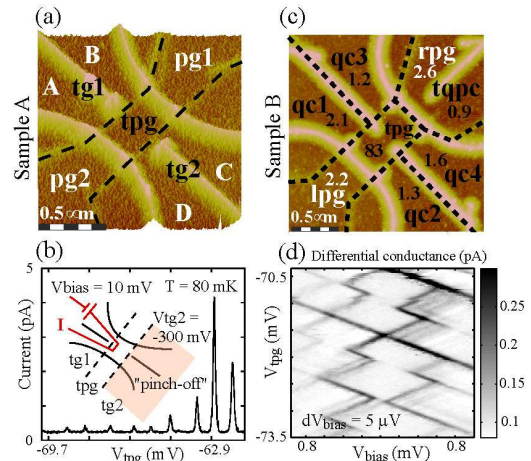
FIG. 2: (a) SFM-micrograph of sample A. The 2DEG is depleted below the oxide lines on the GaAs surface (grey). The Ti film is structured into three isolating parts by Ti-oxide lines (dashed lines). (b) Conductance is measured across the quantum dot of sample A as a function of the top plunger gate (tpg) at 80 mK. (c) SFM-micrograph of sample B. Dashed lines indicate the second pattern in the Ti film with its six top gate segments. The lever arm of the gates on the quantum dot are estimated and quoted in percent (white numbers). (d) Differential conductance of the lower left dot of sample B is measured as a function of voltage bias and top plunger gate voltage.

Sample A is shown in Fig. 2 (a). A quantum dot (QD) structure connected to four distinct leads via quantum point contacts (QPCs) is defined by local oxidation of the GaAs surface (grey lines). This structure with only two in-plane gates does not allow individual tuning of the four QPCs and the dot. A thin Ti film is evaporated onto the structure and segmented by two oxide lines (dashed lines). The QPCs are labelled A,B,C,D (white). The Ti top gate regions are named (black letters) top gate 1 (tg1), top plunger gate (tpg) and top gate 2 (tg2). The in-plane gates formed by regions of the 2DEG next to the QD are labelled (white letters) plunger gate 1 and 2 (pg1 and pg2). Within measurement accuracy we do not observe a change in the QPC conductance at 4.2 K after writing oxide lines in the Ti film on top. The three electrically separated regions of the top gate together with the two in-plane gates give five independent control parameters that can be used to tune the four QPCs and the dot. In addition, the global electron density of the structure can be tuned with the back gate. The separation of the two Ti-oxide lines is less than 290 nm peak-to-peak and and the Ohmic resistance of the top gate tpg bridging the structure is only a few kΩs larger than that of the unpatterned Ti film. In order to demonstrate the functionality of the top and in-plane gates we have measured their action on the conductance of selected QPCs relative to the action of the back gate at

a temperature of 4.2 K. Conductance is measured from QPC A to QPC B by pinching off the two other QPCs with top gate 2. Clear Coulomb blockade is observed (see Fig. 2 (b)) as a function of the top plunger gate at an electronic temperature of about 80 mK.

Sample B is a double QD structure as illustrated in Fig. 2 (c). The dashed black lines indicate the oxide lines in the Ti film, the thick bright lines are those on the GaAs surface. Each of the four QPCs connecting the dots to the leads can be controlled by a separate top gate (qc1...qc4). In addition, two in-plane gates (lpg and rpg) act as plunger gates for the quantum dots. The coupling between the dots can be tuned by the top plunger gate (tpg). The detector QPC flanking the top right QD forms an integrated charge read-out [20]. It is tunable with another top gate region (tqpc).
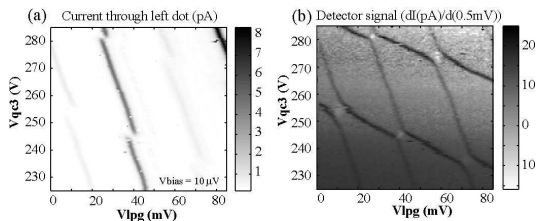
FIG. 3: (a) Conductance through the lower left dot of Fig. 2 (c) is measured as a function of the left in-plane gate V_{lpg} and the top gate segments $V_{qc3} = V_{qc4} + 130\ mV$. (b) The full charge stability diagram of the double dot system is measured in the QPC detector signal.

Coulomb diamonds are shown in Fig. 2 (d) as differential conductance maps measured through the contacts below top gate areas qc1 and qc2. The charging energy of each quantum dot is about 0.5 meV. The lever arms of the gates on the lower left dot in this regime have been measured from Coulomb blockade diamonds as a function of the top plunger gate (see Fig. 2 (d)) and conductance measurements in the parameter plane of the top plunger gate and all other gates. Since the sum of all lever arms is unity, we quote the numbers for individual gates in percent in Fig. 2 (c). The lever arm of the top plunger gate (tpg) is significantly larger than that of all other gates. The lever arms of the quantum point contact top gates (qc1 to qc4) are comparable to those of the in-plane gates (lpg,rpg). The lever arm of the top gate above the detector QPC (tqpc) is the smallest. These findings agree with expectations from the sample geometry.

Figure 3 (a) shows a conductance map for transport through the lower left dot of Fig. 2 (c). The tunnel couplings of the upper right dot are completely pinched off in this regime of voltages applied to gates qc3 and qc4. The data is taken by using qc3 and qc4 as tuning gates with $V_{qc3} = V_{qc4} + 130\ mV$. Dark lines correspond to conductance resonances as a function of the two tuning parameters, the left in-plane gate V_{lpg} and the top gate segments qc3 and qc4.

When the charge detector QPC is tuned into the tunneling regime we are able to detect charging of the individual dots with single electrons [20]. The charge stability diagram of the double dot system with its characteristic hexagon pattern [21] can be mapped out as a function of two tuning gates (see Fig. 3 (b)). The charge detector is closer to the upper right dot in Fig. 2 (c) and therefore shows a stronger signal if this dot is charged. This gives rise to the lines with the smaller slope in Fig. 3 (b) in agreement with the relative location of this dot to the two sets of tuning gates, respectively. The lines with the larger slope and weaker contrast lie exactly on the conductance maxima presented in Fig. 3 (a) reflecting the charging of the dot in the lower left. This demonstrates individual control over nanostructured in-plane and top gate electrodes.

The two structures discussed above demonstrate the functionality of complex coupled nanoscale systems patterned in the Ga[Al]As system with the layer by layer local oxidation technique. The alignment of the pattern in the Ti film relative to the oxide lines on GaAs is straightforward and only limited by the resolution of the SFM. Stable Coulomb peaks demonstrate the high quality of the resulting structures. In addition, these results enable the fabrication of coupled structures and hold promise for innovative designs of highly tunable semiconductor nanostructures.

[1] J.A. Dagata, J. Schneir, H.H. Harary, C.J. Evans, M.T. Postek, and J. Bennet, Appl. Phys. Lett. **56**, 2001 (1990).
[2] M. Wendel, S. Kuhn, H. Lorenz, J.P. Kotthaus, and M. Holland, Appl. Phys. Lett. **65**, 1775 (1994).
[3] S.C. Minne, H.T. Soh, P. Flueckiger, and C.F. Quate, Appl. Phys. Lett. **66**, 703 (1995).
[4] P. Avouris, T. Hertel, and R. Martel, Appl. Phys. Lett. **71**, 285 (1997).
[5] J. Shirakashi, K. Matsumoto, N. Miura, and M. Konagai, Appl. Phys. Lett. **72**, 1893 (1998).
[6] J.C. Rosa, M. Wendel, H. Lorenz, J.P. Kotthaus, M. Thomas, and H. Kroemer, Appl. Phys. Lett. **73**, 2684 (1998).
[7] L.P. Rokhinson, D.C. Tsui, L.N. Pfeiffer, and K.W. West, Superl. Microstr. **32**, 99 (2002).
[8] M. Ishii and K. Matsumoto, Jpn. J. Appl. Phys. **34**, 1329 (1995).
[9] R. Held, T. Heinzel, P. Studerus, K. Ensslin, and M. Holland, Appl. Phys. Lett. **71**, 2689 (1997).
[10] S. Lüscher, A. Fuhrer, R. Held, T. Heinzel, K. Ensslin, and W. Wegscheider, Appl. Phys. Lett. **75**, 2452 (1999).
[11] U.F. Keyser, H.W. Schumacher, U. Zeitler, R.J. Haug, and K. Eberl, Appl. Phys. Lett. **76**, 457 (2000).
[12] A. Fuhrer, A. Dorn, S. Lüscher, T. Heinzel, K. Ensslin, W. Wegscheider, and M. Bichler, Superl. Microstr. **31**,

19 (2002).

[13] R. Nemutudi, C.G. Smith, C.J.B. Ford, N.J. Appleyard, M. Pepper, D.A. Ritchie, and G.A.C. Jones, J. Of Vacuum Science and Technology B . **20**, 2810 (2002).

[14] H. Sugimura, T. Uchida, N. Kitamura, and H. Masuhara, Appl. Phys. Lett. **63**, 1288 (1993).

[15] B. Irmer, M. Kehrle, H. Lorenz, and J.P. Kotthaus, Appl. Phys. Lett. **71**, 1773 (1997).

[16] R. Held, S. Lüscher, T. Heinzel, K. Ensslin, and W. Wegscheider, Appl. Phys. Lett. **75**, 1134 (1999).

[17] K. Matsumoto, M. Ishii, K. Segana, Y. Oka, B.J. Vartanian, and J.S. Harris, Appl. Phys. Lett. **68**, 34 (1996).

[18] T. Heinzel, R. Held, S. Lüscher, T. Vancura, K. Ensslin, T. Blomqvist, I. Zozoulenko, and W. Wegscheider, Advances in Solid State Physics **39**, 161 (1999)

[19] M.C. Rogge, C. Fühner, U.F. Keyser, R.J. Haug, M. Bichler, G. Abstreiter, and W. Wegscheider, Appl. Phys. Lett. **83**, 1163 (2003).

[20] M. Field, C.G. Smith, M. Pepper, D.A. Ritchie, J.E.F. Frost, G.A.C. Jones, and D.G. Hasko, Phys. Rev. Lett. **70**, 1311 (1993).

[21] C. Livermore, C.H. Crouch, R.M. Westervelt, K.L. Campman, and A.C. Gossard, Science **274**, 1332 (1996).